Materials Science Forum *Online: 2009-12-03*
ISSN: 1662-9752, Vol. 635, pp 175-180
doi:10.4028/www.scientific.net/MSF.635.175

Thermodynamic Modelling of Ferromagnetic Shape Memory Actuators

Berthold Krevet[1], Manfred Kohl[1,2]
[1] *Forschungszentrum Karlsruhe, IMT, Postfach 3640, 76021 Karlsruhe, Germany*
[2] *University of Karlsruhe, IMT, Kaiserstr. 12, 76131 Karlsruhe, Germany*

Keywords*:* Ferromagnetic shape memory alloys, finite element simulation, Gibbs potential, magnetic anisotropy.

Abstract
We present a thermodynamic Gibbs free energy model for the finite element simulation of the coupled thermo-magneto-mechanical behavior of ferromagnetic shape memory alloys (FSMAs). Starting from a free energy model for the conventional shape memory effect, additional terms are included to take into account the magnetic anisotropy and the geometry-dependent magnetostatic energy. Different functions are considered for the strain dependence of the anisotropy energy in order to describe the experimentally found strong dependence of the anisotropy energy on the ratio of short and long crystallographic axis *c/a*. The resulting energy landscape is used to calculate the transition probabilities between three martensite variants and the austenite state under applied stress and external magnetic field. The magnetic shape memory effect is simulated for different loading conditions and sample geometries. We demonstrate the influence of the *c/a* dependence of the anisotropy energy as well as the influence of twinning strain and elastic modulus on the transition between martensite variants. The model calculations are compared with experimental results on Ni-Mn-Ga single crystals.

Introduction

Ferromagnetic shape memory alloys (FSMAs) like Ni-Mn-Ga generate large strokes in the presence of moderate magnetic fields [1], which opens up the development of a new class of actuator devices. In particular, the option of contactless control of large deformations at relatively large bandwidths is an important prerequisite for applications in micro-electro-mechanical systems (MEMS). The design of FSMA actuators requires a deep understanding of magneto-mechanical coupling effects depending on material parameters, geometry and loading conditions. Different modeling approaches have been developed up to now, which either focus on a thermodynamic analysis [2,3] or on a phenomenological description [4].
Recently, a free energy model of the shape memory effect given in [5] has been combined with a Stoner-Wohlfarth model of magnetic anisotropy to describe the evolution of martensite variants as a function of stress and magnetic field [6]. The model has been implemented in a finite element (FEM) program for the simulation of coupled magneto-mechanical field problems. First simulations based on this model reproduce the basic features of the magnetic shape memory effect [6]. Further model extensions include the phase transition between austenite and martensite variants in a magnetic field under different loading conditions [7].
Up to now, the saturation magnetization and magnetic anisotropy energy Ku are considered to be constant. However, experimental evidence suggests that Ku depends on the ratio of short and long crystallographic axis *c/a* [8]. Therefore, a strain dependence of Ku is assumed in order to investigate possible effects on the reorientation of martensite variants. In addition, the low elastic modulus derived from detwinning experiments, $E_{tw}=\sigma_{tw}/\varepsilon_{tw}$ is distinguished from the elastic modulus E_M derived from deformation experiments on a detwinned sample, e.g., from compression along the c axis. In the following, it is demonstrated that these model extensions allow the simulation of magnetic field induced strain (MFIS) measurements on bulk Ni-Mn-Ga samples [9,10], which largely differ by their twinning strain and elastic modulus as well as their stress dependence of MFIS.

The FSMA model

Starting point is the Müller-Achenbach-Seelecke model for the transition (reorientation) between two martensite variants M^- and M^+ with short and long axes c and a, respectively, being oriented along the beam axis [5]. The difference between the crystallographic axis *c-a* is due to a negative and positive eigenstrain ε_T. In this model, the transition is considered as a thermally activated process, which describes the switching of the variants in an energy landscape with two energy wells and one maximum between the wells [5]. From the relative phase fractions x^- and x^+ of the variants under different loading conditions the stress-strain relation can be derived.
The two-variant-model has been extended to a three-variant-model according to Fig. 1a to account for the magnetic field-induced reorientation [6]. Fig. 1b shows the coordinate system of the test beam used for the calculations. For each combination of variant transitions a free energy model is constructed. Fig. 3 shows the Helmholtz free energy ψ as function of strain ε consisting of five piecewise parabolic functions of ε. It is suitable to describe the transition between variants M1 and M2 with the relative fractions X1 and X2:

$$\begin{aligned}
\psi_1(\varepsilon) &= E_M/2\,(\varepsilon+\varepsilon_T)^2 && \text{if } \varepsilon < -\varepsilon_T,\\
\psi_2(\varepsilon) &= E_{tw}/2\,(\varepsilon+\varepsilon_T)^2 && \text{if } -\varepsilon_T < \varepsilon < -\varepsilon_M\\
\psi_3(\varepsilon) &= E_{Tw}/2\,(\varepsilon_M-\varepsilon_T)\,\varepsilon^2/\varepsilon_M-\varepsilon_T) && \text{if } -\varepsilon_M \le \varepsilon \le \varepsilon_M\\
\psi_4(\varepsilon) &= E_{tw}/2\,(\varepsilon-\varepsilon_T)^2 && \text{if } \varepsilon_M < \varepsilon < \varepsilon_T\\
\psi_5(\varepsilon) &= E_M/2\,(\varepsilon-\varepsilon_T)^2 && \text{if } \varepsilon_T < \varepsilon
\end{aligned} \qquad (1)$$

ε_M defines the stress, at which the transition starts. It is connected to the twinning strain ε_{tw} by:

$$\varepsilon_{tw} = \varepsilon_T - \varepsilon_M \qquad (2)$$

E_M is the elastic modulus calculated from compression or tensile experiments on samples, which are in a single variant state with the applied force being parallel to the c-axis or a axis, respectively. E_{tw} is the elastic modulus, which is derived from detwinning measurements showing variant reorientation. $\psi_1(\varepsilon)$ describes the situation of compression of variant M1 along the direction of principal stress (x-direction). $\psi_2(\varepsilon)$ describes the situation of tensile loading and $\psi_3(\varepsilon)$ the transition region from variant M1 to M2. The situation of compression of variant M2 is described by $\psi_4(\varepsilon)$. The tensile loading of M2 is described by $\psi_5(\varepsilon)$. The elastic modulus E_M is assumed to be in the order of 2 GPa, which is much larger than E_{tw} being in the order of 50 MPa.

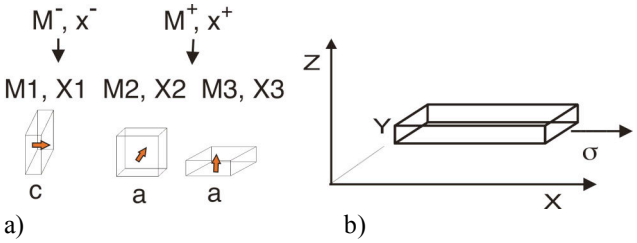

Fig. 1 a): Extension from the two-variant model to the three-variant model. The magnetic moment is aligned to the c-(short) axis.
b) : Geometry of a test beam used for the simulations.

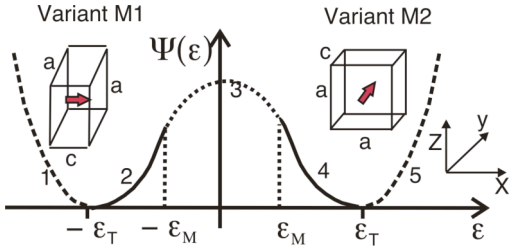

Fig. 2: Parabel model for the free energy to describe the transition from variant M1 to variant M2. The magnetic moment rotates in the x-y plane

In the model, the twinning stress does not enter explicitly, it is given by the product of ε_{tw} and E_{tw}. For prescribed stress σ, the equilibrium condition is determined by the minimum condition of the Gibbs free energy g, which is related to ψ by a Legendre transformation with respect to σ :

$$g = \psi - \sigma\,\varepsilon \qquad (3)$$

To construct the Gibbs potential $g(\varepsilon,\alpha,\sigma,B)$ in the magnetic field B, the magnetic anisotropy energy Ku, the Zeeman energy E_z and the magneto-static energy F_m must be added. In the following model, the angle α defines the rotation of the magnetic moment M_s by the external

field B with respect to the easy axis of variant M1 and α_σ defines the angle between the easy axis of variant M2 or M3 with respect the easy axis of M1. Then the anisotropy contribution Ku to the Gibbs potential is given by:

$$Ku = K*\sin(\alpha_\sigma - \alpha)^2, \quad (4)$$

$\alpha_\sigma = 0$ if $\varepsilon < 0$ and $\alpha_\sigma = \pi/2$ if $\varepsilon > 0$.

The Zeeman energy is given by:

$$E_z = - M \cos(\alpha_B - \alpha)B \quad (5)$$

Where α_B is the angle of the magnetic field with respect to the easy axis of variant X1.

The free energy distribution from the magneto-static interaction is given by:

$$F_m = - \int 1/2\ \mu_0\ \mathbf{MH_m}\ dV \quad (6)$$

H_m is the field created by the magnetization M. It is connected to M by the demagnetization tensor N in the case of a homogeneous field $\mathbf{H_m}$:

$\mathbf{H_m} = - N * \mathbf{M}$

For the transition between variant M1 and M2 this reduces to

$$F_m = 1/2\ \mu_0\ M^2\ (N_x \cos(\alpha)^2 + N_y \sin(\alpha)^2) \quad (7)$$

N_x and N_y are the demagnetization coefficients in x and y direction, respectively.

To calculate the transition probabilities p^{ij} between the variants Mi and Mj, the position $P_i(\varepsilon,\alpha)$ and $P_j(\varepsilon,\alpha)$ of the two minima g^i and g^j of g $(\varepsilon,\alpha,\sigma,B)$ in the ε-α plane are determined numerically. We assume that the transition follows a straight line from P_i to P_j in the $\alpha-\varepsilon$ plane and take for the barrier high g^{ij} the maximum of g along this path. With the two constants A and V, the transition probabilities are given by:

$$p^{ij} = A \exp(-(g^{ij}-g^i)V/k_BT), \qquad p^{ji} = A \exp(-(g^{ij}-g^j)V/k_BT) \quad (8)$$

These expressions are used to solve the rate equations for the variant fractions X1 and X2, from which the total strain ε, the stress σ and the magnetization M are derived [6,7].

In this model, for the transition from variant 1 to 2, it is assumed, that variant 1 is first strained towards lower eigenstrain and when this strain is equal to ε_M, the transition to variant 2 occurs. When a variant is deformed to a more cubic state, the anisotropy energy should be reduced [8]. At $\varepsilon=0$ variant M1 and M2 cannot be distinguished. However the magnetic anisotropy energy gives different contributions for M1 and M2 to the Gibbs potential and therefore should vanish at $\varepsilon=0$. In this paper we replace Ku by the following two functions, which fulfill these requirements:

$$K^1u(\varepsilon): K\ (1-\exp(-2\varepsilon^2/\varepsilon_T^2)) = K*f1(\varepsilon) \quad (9a)$$

$$Ku^2(\varepsilon) : K\ ((1-\exp(-\varepsilon^2/\varepsilon_T 2))/0.632) = K*f2(\varepsilon) \quad (9b)$$

Function f1 gives only a weak dependence near ε_T and resembles the assumption of a constant Ku of previous models, whereas f2 leads to an almost linear decrease at ε_T and is similar to the results reported in [8]. Both function vanish at $\varepsilon=0$.

Model features

For all simulations reported in this paper the magnetic field is applied in y-direction. Thus the field induces the transition from variant M1 to M2. E_M is set to 2 GPa, K to 1.7 MPa and ε_T to 0.035. For the saturation Magnetization M_s a value of 6.5 T is used. The saturation field strength of the easy axis is set to 0.05 T.

For the following simulations the assumed sample dimension is $l_x*l_y*l_z = 9*9*3\ mm^3$. To reduce the influence of the magneto static energy on the variant transition, the sample length in x and y

direction are chosen to be equal. The constants A and V are set to 10^3 s^{-1} and $5*10^{-23}$ m^3 respectively. For all simulations room temperature (293 K) is assumed.

Strain dependence of Ku. The two functions f1 and f2 used for the strain dependence of Ku are plotted in Fig. 2. Their influence of the Gibbs potential $g(\alpha,\varepsilon)$ is shown in the Figs. 4 and 5 for the case of external field strength B_y = 0.4 T and zero bias stress. A much stronger decrease of the Gibbs potential with increasing ε in the vicinity of $-\varepsilon_T$ can be seen in the case of f2. This favors the transition from variant M1 to variant M2.

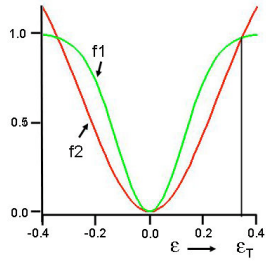

Fig.3 The functions f1 and f2 versus strain.

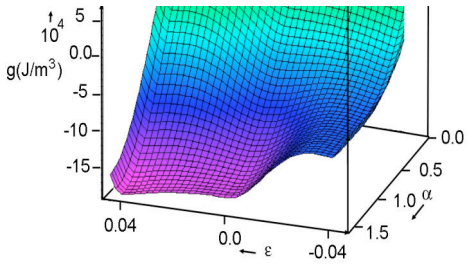

Fig. 4: Gibbs potential as fuction of ε and α using f1 for Ku. B_y=0.4 T, ε_T = 0.038, bias stress = 0 MPa.

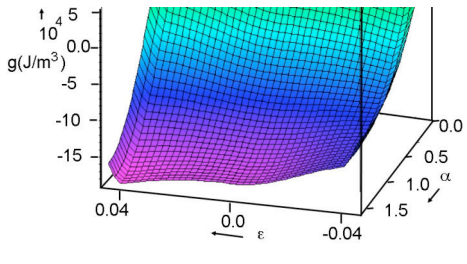

Fig. 5: Gibbs potential as fuction of ε and α using f2 for Ku. B_y=0.4 T, ε_T = 0.038, bias stress = 0 MPa.

The influence of f1 and f2 on the magnetization characteristic at different bias stress is shown in Fig. 6 for increasing magnetic field B_y. The simulation parameters are: E_{tw} = 50 MPa, ε_{tw} = 1 %. The jump in the magnetization curve from the hard axis values to the easy axis is due to the transition from variant M1 to M2. Using function f2 the transition starts at lower fields for all bias stresses except for zero stress, where no difference is found between f1 and f2.

When the field is decreased no differences are found between f1 and f2. The reason is that for variant M2 the anisotropy energy is zero for a magnetic field in y-direction ($\alpha = \alpha_\sigma = \pi/2$) and thus the special function used for Ku(ε) will not influence the Gibbs potential of M2.

Effect of twinning strain. The magnetization characteristic as a function of B_y for different assumed twinning strains is shown in the Fig. 7 for a bias- stress of 1.5 MPa. The corresponding values of the elastic modulus E_{tw} are set to be consistent with a twinning stress of 1 MPa. For increasing field the transition starts first in the case ε_{tw} = 1%. The reason is the reduced barrier height due to the low elastic modulus (100 MPa). When the field is decreased, reorientation to variant M1 occurs first in the case ε_{tw} = 0.2%. At zero bias stress a difference is only found for increasing B_y in the case ε_{tw} = 1 %: The transition to variant M2 starts at a field strength of 0.1 T, which is by 0.1 T lower compared to the cases ε_{tw} = 0.05 % and ε_{tw} = 0.2%. The results demonstrate, how variant reorientation is affected by both, ε_{tw} and E_{tw} and not only by their product.

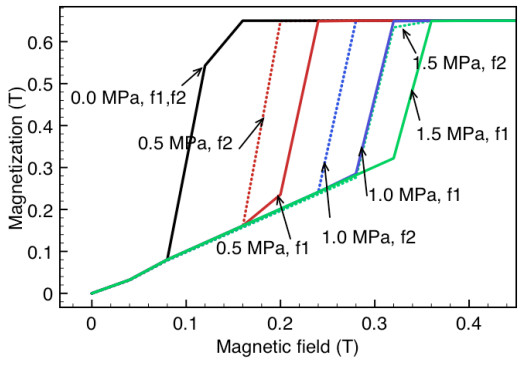

Fig. 6: Magnetization- magnetic field characteristic for the two functions f1 and f2 for increasing magnetic field.

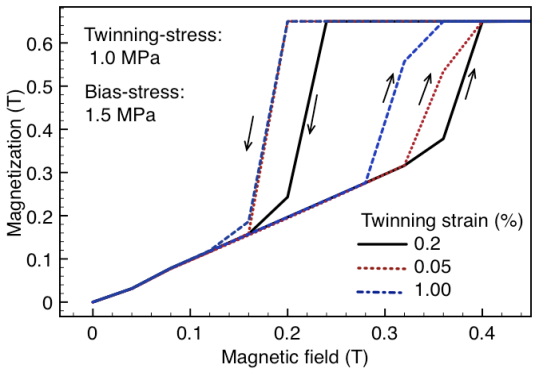

Fig. 7: Magnetization-magnetic field characteristic at a bias-stress of 1.5 MPa for different values of ε_{tw}.

Comparison with experiment. The model is used to reproduce the magnetic field induced strain of two different Ni-Mn-Ga samples, reported in the literature. Their main material parameters and the geometry are summarized in table 1. In the case of sample 1 [9] the material parameters are chosen to fit the experiments, in the case of sample 2 [10] they are derived from the measured stress-strain characteristic. The MFIS for sample 1 and 2 are shown in Fig. 9 and 10, respectively. Sample 1 is more robust against the bias-stress. No marked attenuation of the MFIS is found up to 1.5 MPa and the limiting stress value for complete variant reorientation in decreasing field is about 1 MPa. In contrast sample 2 shows a considerable reduction of the MFIS at 1.0 MPa. In this case a reversible transition occurs in the field range of 0.15-0.5 T.

Sample 1

E_{tw} = 500 MPa
E_M = 2.0 GPa
ε_{tw} = 0.2%
lx*ly*lz: 3.5*2*0.5 cm^3

Sample 2

E_{tw} = 50 MPa
E_M = 2.0 GPa
ε_{tw} = 1.0%
$l_x*l_y*l_z$ = 9*5*3 mm^3

Table 1: Characteristic features of the two samples.

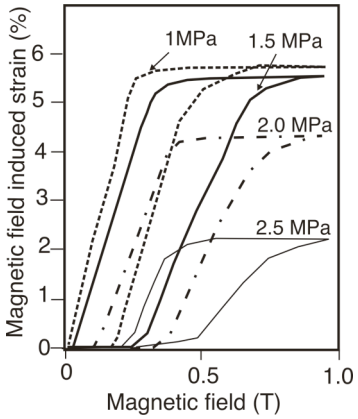

Fig. 8: Strain versus applied magnetic field B_y at different bias-stress for sample1.

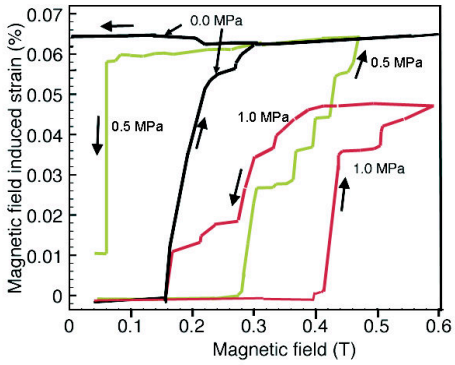

Fig. 9: Strain versus applied magnetic field B_y at different bias-stress for sample 2.

Figs. 10 and 11 show the corresponding simulation results of the MFIS for sample 1 and 2, respectively, while Fig. 12 and 13 show the simulated evolution of the phase fraction X2 versus the magnetic field at different bias-stress. For the simulations the function f2 is used. The sharp transitions in the simulation are due to the assumption of a perfectly homogeneous single crystal. In the case of sample 1 the MFIS is nearly unaffected up to 1.5 T. A sharp decrease occurs above 2.3 MPa. Fig. 12 shows that the corresponding phase fraction X2 saturates at a value of 0.38. Therefore we conclude that the decrease of the MFIS is due to this incomplete transition. In contrast sample 2 shows a full transition for all simulated bias stresses (Fig. 13). The decrease of MFIS with increasing bias stress, shown in Fig. 11, is caused by the large deformation of the material due to the low value of elastic modulus E_{tw}.

Neglecting the difference between E_M and E_{tw} would result in large negative strain values due to the bias-stress if variant M1 is in the order of 1.

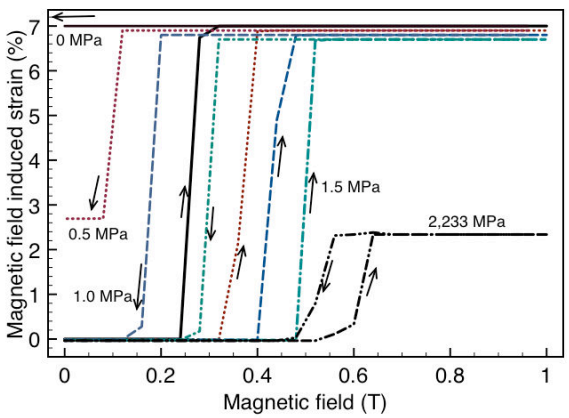

Fig. 10: Simulated strain versus magnetic field at different bias-stress for sample 1.

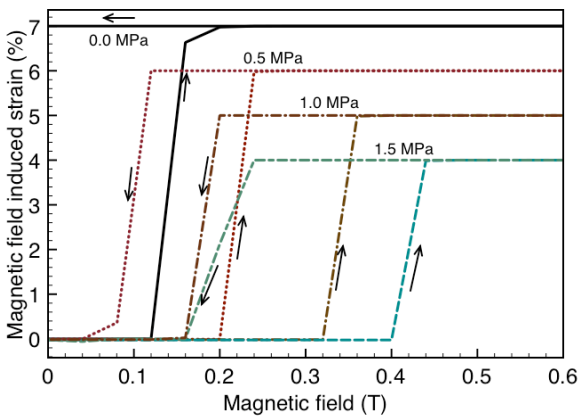

Fig. 11: Simulated strain versus magnetic field at different bias-stress for sample 2.

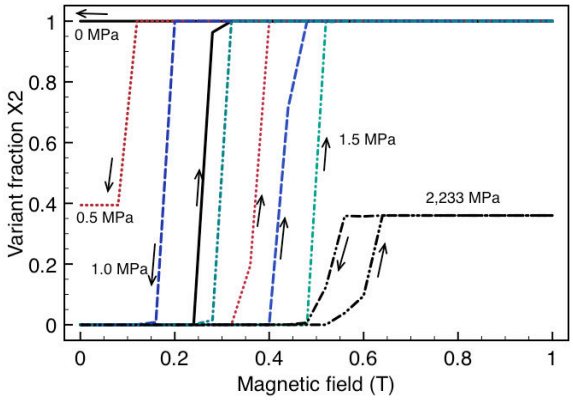

Fig. 12: Variant fraction X2 versus magnetic field for sample 1 at different bias-stress.

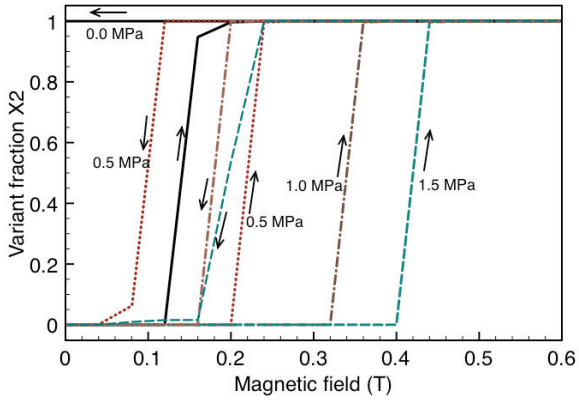

Fig. 13: Variant fraction X2 versus magnetic field for sample 2 at different bias-stress.

Conclusion

A free energy function and the resulting Gibbs potential are constructed to describe magnetic-field and stress-dependent reorientation of martensite variants. Two different values of the elastic modulus E_M and E_{tw} are used to describe the stress strain relations. The model allows the simulation of the stress and field dependence of MFIS covering a broad range of FSMA materials, which are currently investigated in experiments. The main results are: a) ε_{tw} and E_{tw} are required for an adequate description of the critical field for MFIS, b) for large values of E_{tw}, MFIS is only reduced is due to incomplete variant transformation, whereas for low values of E_{tw}, MFIS mainly decreases due to the large deformation, c) the strain dependence of Ku is explicitly included in the model, which has a significant influence on the critical magnetic field of MFIS. The simulations reproduce the main features of the experimental results.

References

[1] K. Ullakko, J. K. Huang, C. Kantner, R. C. O´Handley, V. V. Kokorin, Appl. Phys. Lett 69 (1996.), 1967

[2] R. D. James, M. Wuttig, Philos. Mag. A77, (1998) 1273 – 1299.

[3] R. C. O´Handley, J. Appl. Phys. 83, (1998) 3263 – 3266.

[4] V. A. L'vov, E. V. Gomonaj, V. A. Chernenko, J. Phys: Condens. Matter 10 (1998) 4587 – 4595).

[5] S. Kim, S. Seelecke, Int. journal of SOLIDS and STRUCTURES, 44 (2007), 1196-1209.

[6] B. Krevet, M. Kohl, P. Morrison and S. Seelecke, Eur. Phys. J. Special Topics 158, 205-211 (2008).

[7] B. Krevet, M. Kohl and S. Seelecke, Proc. ICOMAT 08, Santa Fe, USA, (2008).

[8] A. Sozinov, A. A. Likhachev, and K. Ullakko, IEEE TRANSACTIONS ON MAGNETICS, VOL. 38, NO. 5, pp. 2814-2816, Sept. 2002.

[9] J. Tellinen, I. Suorsa, A. Jääskeläinen, I. Aaltio and K. Ullakko, 8th international conference ACTUATOR 2002, Bremen, Germany, 10-12 June 2002.

[10] K.Rolfs, A. Mecklenburg, J.-M. Guldbakke, R.C. Wimpory, A. Raatz, J. Hesselbach and R.Schneider, J. Magn. Magn. Mater. (2008), doi:10.1016/j.jmmm.2008.10.023.